water

MDPI

Article

Estimating Sediment Flushing Efficiency of a Shaft Spillway Pipe and Bed Evolution in a Reservoir

Ching-Nuo Chen [1,*] and Chih-Heng Tsai [2]

[1] International Master Program of Soil and Water Engineering, National Pingtung University of Science and Technology, Pingtung 91201, Taiwan
[2] Department of Recreation and Healthcare Management, Chia Nan University of Pharmacy and Science, Tainan 71710, Taiwan; jht581212@gmail.com
* Correspondence: ginrochen@mail.npust.edu.tw

Received: 9 October 2017; Accepted: 22 November 2017; Published: 28 November 2017

Abstract: Control of reservoir sedimentation in order to ensure their sustainable use has drawn attention among water engineers and water resource managers. Several methods have been proposed, but most of the developed methodologies are incapable of modelling bed evolutions, while at the same time, compute sediment flushing efficiency. In this study a two-dimensional bed evolution model is proposed to estimate sediment distribution, bed evolution and sediment flushing efficiency of reservoirs. A-Gong-Dian reservoir, in southern Taiwan, is used as an illustrative example. Typhoon events were used to verify the proposed model. Simulations were conducted for one and two-day storm events under return periods, 2, 5, 10, 25, 50, 100, and 200-year. The results indicated that the average sediment flushing efficiency of the shaft spillway under one and two-day storms were close, 58.50% and 59.39%, respectively. These results were similar to observed laboratory tests experiments, where an efficiency of 65.34% was obtained. This study suggests that the applied model could be adopted to ensure the sustainable use of reservoirs, and also to find an optimal area for the location of a shaft spillway pipe. Therefore, the proposed model could serve as a reference to the reservoir management personnel.

Keywords: two-dimensional bed evolution model; sediment flushing of empty storage; shaft spillway pipe; sediment flushing efficiency

1. Introduction

Reservoirs are often affected by accelerated sediment deposition rates and has shortened the life of reservoirs by more than 65% in China alone [1]. As a result, the economic value of such projects has severely declined. Not only do they influence the life of reservoirs, they also pose safety hazards, as illustrated by [2]. Their sustainability is strongly dependent on how well the rate of sediment deposition is reduced and on the techniques of managing the reservoirs. Several techniques are available for their management, amongst which are mechanical excavation, dredging (conventional dredging, dry excavation), and hydraulic desilting. For an exhaustive review of the different techniques, the reader is referred to [3], who explored sustainable sediment management in reservoirs based on experience from five continents. Mechanical excavation and dredging boats, however, are associated with higher costs when compared to hydraulic desilting, and are often plagued by subsequent disposal problems. Hydraulic desilting employs stream power and hydraulics to cut down sediment deposits downstream. Flushing out sediments in reservoirs has been shown to cut costs [4], despite the large amount consumed by the flushing operations. Emamgholizadeh and Samadi [5] classify flushing into two, complete (also termed empty) and partial drawdown flushing. These, in turn, include hydro-suction, sediment sluicing, sediment bypass, density current venting, and hydraulic flushing through the reservoir, used independently or in combination [6]. The efficiency of sediment flushing depends on the geometry of the reservoir, sediment particle size, characteristics of sediments deposited, flow discharge, and flow depth. Several authors have argued that the efficiency of sediment flushing is influenced by the ratio of storage volume to incoming runoff [7], which should be less than 0.05 [8] for this technique to work. Moreover, we did not evaluate this threshold in this study, since the reservoir under investigation already applied hydraulic sediment flushing. Madadi, et al. [9] managed to improve flushing efficiencies by up to 280% through reconfigured reservoir bottom outlets in laboratory experiments.

Effective management of reservoirs system require a model that can predict future behaviour and response to perturbation [10], and all of the models are developed through experiments and depending on the status quo, they may grow in complexity to include conceptual frameworks, computer calculations, numerical simulations, and physical scale modelling [11]. Physical models have been applied to study the process and efficiency of sediment flushing in a reservoir. Although they have been successfully used to understand and reproduce to some extent complex physical processes that occur in nature, and have contributed significantly in hydraulic construction designs, they are relatively costly and time consuming [12]. More recently photogrammetry-based surveys using unmanned aerial systems have been used to evaluate flushed sediments [13–15]. Moreover, such techniques can only compute the amount of flushed sediments only when the reservoir is dry (i.e., empty), and subsequent images are necessary to compute the Digital Elevation Models (DEMs) of difference, from which the flushing efficiencies may be computed. Network-based programming techniques have also been employed in multi-reservoir systems [16], though their core emphasis is on determining empty flushing of sediments.

Given the recent advances in computational power, multi-dimensional models have increased the capability of assessing sedimentation problems and the multi-dimensional models have been extensively adopted in engineering application and analysis. For models to be adopted, they should reflect the physical characteristics of the reservoir and complexity in question. Numerical sediment transport models are available in one, two, and three dimensions. The widely used models, however, are one- (1D) and two-dimensional (2D) models when compared to the high computer intensive three-dimensional (3D) models. Examples of 1D sediment transport models are HEC-6 [17], HEC-RAS [18], and FLUVIAL-12 [19,20]. Castillo, Carrillo, and Álvarez [7] employed four complementary methods, which included 1D model, to determine sedimentation and flushing in a reservoir These models are capable of simulating longitudinal flows in rivers, moreover, they run short in the simulation of sediment transport and bed evolution in reservoirs. To be applied in sediment flushing, several assumptions should be made, thus, compromising the accuracy and efficiency in reservoir management. In such situations, reservoirs are narrow in shape, flow highly channelized, while closely following the thalweg [12]. However, most reservoir pools are wide and have no single clear flow direction, and they often constitute complex topography and geometry. As a result, multi-dimensional models are used. Olsen [21] used a depth-averaged 2D model to study the flushing process in a water reservoir in Nepal. Besides two-dimensional models, three-dimensional models have also been applied to study sediments in reservoirs. Olsen and Skoglund [22] applied a 3D model to calculate the sediment deposition in a hydropower reservoir, and also in a sand trap. Fang and Rodi [23] used a 3D model to simulate flow and sediment transport in the Three Gorges Project (TGP) reservoir in Yangtze River. Khosronejad, et al. [24] used a three-dimensional finite volume model to study the effects of various parameters on the quantity of sediment that was released from a reservoir in the reservoir flushing process.

Although the above models could estimate sediment erosion and deposition, bed evolution in a reservoir, and the efficiency of flushing, we have not found a model that is capable of combining all of these key reservoir management strategies in a single package. In addition, the above stated models require suspended sediment concentration, and sediment yield hydrograph into the reservoir, which are not easily obtained. Consequently, rating curves of discharge and suspended sediment transport rate are used, and these are associated with high errors [25]. Incorrect estimation of sediment inflow into reservoirs especially during flood events, will eventually lead to inefficient flushing of sediments and to misleading bed evolution in the reservoirs. It is therefore imperative to develop models that are highly efficient in estimating inflow hydrographs and sedigraphs, in turn, correctly estimating the amount of sediments to be flushed, while estimating the resultant bed evolution. A two-dimensional bed evolution model having these capabilities is developed and applied in this study. The upstream boundary condition hydrographs of inflow discharge and suspended sediment concentration for the 2D dimensional bed evolution model were calculated by the Physiographic Soil Erosion and Deposition (PSED) [26]. The PSED model can accurately estimate discharge hydrographs, concentration of suspended sediment hydrograph and suspended sediment transport rate from a watershed.

2. Numerical Model

The depth-averaged two-dimensional bed evolution model is divided into three parts: (1) water flow calculations; (2) sediment transport calculations; and, (3) bed elevation variation calculations.

2.1. Governing Equations for Water

The depth-averaged continuity and momentum equations are given below:

$$\frac{\partial h}{\partial t} + \frac{\partial (uh)}{\partial x} + \frac{\partial (vh)}{\partial y} = 0 \tag{1}$$

$$\frac{\partial (uh)}{\partial t} + \frac{\partial (uuh)}{\partial x} + \frac{\partial (uvh)}{\partial y} = \frac{\partial}{\partial x}\left(2\varepsilon h \frac{\partial u}{\partial x}\right) + \frac{\partial}{\partial y}\left[\varepsilon h \left(\frac{\partial u}{\partial y} + \frac{\partial v}{\partial x}\right)\right] - \frac{\tau_{bx}}{\rho} - gh\frac{\partial H}{\partial x} \tag{2}$$

$$\frac{\partial (vh)}{\partial t} + \frac{\partial (vuh)}{\partial x} + \frac{\partial (vvh)}{\partial y} = \frac{\partial}{\partial x}\left[\varepsilon h \left(\frac{\partial u}{\partial y} + \frac{\partial v}{\partial x}\right)\right] + \frac{\partial}{\partial y}\left(2\varepsilon h \frac{\partial v}{\partial y}\right) - \frac{\tau_{by}}{\rho} - gh\frac{\partial H}{\partial y} \tag{3}$$

in which t is time; x and y are horizontal Cartesian coordinates; h is the depth; u and v are depth-average flow velocities in x and y directions; H is water surface elevation; g is gravitational acceleration; ρ is density of flow; ε is the depth-average kinematic eddy viscosities of water; and, τ_{bx} and τ_{by} are bed shear stresses τ_b in x and y directions, $\tau_b = \rho g h S_f$, S_f is the friction slope.

The depth-average kinematic eddy viscosities of water can be approximated and expressed as [27]:

$$\varepsilon = \frac{\kappa}{6} u_* h \tag{4}$$

in which κ is the von Karman constant, and $\kappa = 0.4$ is chosen in this study. u_* is the shear velocity and $u_* = \sqrt{ghS_f}$.

2.2. Governing Equations for Sediment Transport with Source Terms

The convective-diffusive equation of suspended sediment, can be expressed as [28]:

$$\frac{\partial (Ch)}{\partial t} + \frac{\partial (uCh)}{\partial x} + \frac{\partial (vCh)}{\partial y} = \frac{\partial}{\partial x}\left(\varepsilon \frac{\partial C}{\partial x}\right) + \frac{\partial}{\partial y}\left(\varepsilon \frac{\partial C}{\partial y}\right) + q_{se} - q_{sd} \tag{5}$$

where C is the depth-averaged volumetric concentration of suspended sediment; q_{se} and q_{sd} are the entrainment and deposition terms of river bed, respectively. According to Itakura and Kishi [29], the entrained rate of channel bed can be expressed as:

$$q_{se} = 0.008\sqrt{sgd}\left[0.14\frac{\rho}{\rho_s}\left(14\sqrt{\tau_*} - \frac{0.9}{\sqrt{\tau_*}}\right) - \frac{\omega_s}{\sqrt{sgd}}\right] \tag{6}$$

in which $s = (\rho_s - \rho)/\rho$ is the submerged specific gravity of the sediment; ρ_s is density of the sediment; d is diameter of the sediment; ω_s is fall velocity of the sediment; and, τ_* is non-dimensional bed shear stress, $\tau_* = {u_*}^2/sgd$.

The deposition rate of suspended sediment can be expressed as:

$$q_{sd} = \omega_s\, C_a \tag{7}$$

where, C_a is the concentration of sediment near the channel bed. C_a can be estimated from the volumetric concentration of suspended sediment obtained at 0.05 depth from the channel bed. Using the exponential law, the volumetric concentration of suspended sediment may be expressed as [30]:

$$C_a = \frac{P_e}{[\,1 - \exp\,(-P_e)\,]}\, C \tag{8}$$

where P_e is the Peclet's number, which may be expressed as $\omega_s h/\varepsilon$.

An extensively used bed load transport formula is the Meyer Peter and Muller formula (MPM) [31]. Moreover, Wong and Parker [32] amended the MPM formula, and more accurate estimates of bed load transport rate were obtained. Nonetheless, since the original MPM formula is relatively easy to apply when establishing a numerical model, bed load transport was calculated using the original MPM formula in this study.

$$(\frac{k_n}{k'})^{\frac{3}{2}} \gamma h S_f = 0.047(\gamma_s - \gamma)d + 0.25(\frac{\gamma}{g})^{1/3} \left(\frac{\gamma_s - \gamma}{\gamma}\right)^{2/3} {q_b}^{2/3} \tag{9}$$

where γ and γ_s are the specific weight of water and the specific weight of sediment, respectively; q_b is the bed load transport rate per unit width of bed; k_n is Strickler's roughness coefficient, which can be represented as the reciprocal of Manning's roughness coefficient; and, $k' = 26/d_{90}^{1/6}$, d_{90} is the size of sediment in the unit of meter for which 90% of the material is finer.

2.3. Governing Equations for Bed Variation

The bed evolution due to sediment transport rate is not equal throughout an alluvial river. The continuity equation for bed elevation variations can be written as [33,34]:

$$\frac{\partial z}{\partial t} + \frac{1}{1-\lambda}\left[\frac{\partial q_{bx}}{\partial x} + \frac{\partial q_{by}}{\partial y} + (q_{se} - q_{sd})\right] = 0 \tag{10}$$

where z is the channel bed elevation; λ is the porosity, $\lambda = 0.245 + 0.0864/{d_m}^{0.21}$, d_m is the mean sediment diameter [35]; and, q_{bx} and q_{by} are the components of q_b in x and y directions, respectively.

2.4. Numerical Scheme

MacCormack explicit finite-difference method [36] is adopted and is divided into predictor and corrector steps. The forward finite-difference is used to discretize the predictor step while the backward finite-difference is used to discretize the corrector step.

The forward finite-difference is used to compute the water depth h by the continuity equation (Equation (1)) and the u and v are computed by the momentum equations (Equations (2) and (3)). The predicted value may be written as:

$$h^*_{i,j} = h^n_{i,j} + \Omega'_{hf} \tag{11}$$

$$u^*_{i,j} = u^n_{i,j}\frac{h^n_{i,j}}{h^{n+1}_{i,j}} + \Omega'_{uf} \tag{12}$$

$$v_{i,j}^{*} = v_{i,j}^{n} \frac{h_{i,j}^{n}}{h_{i,j}^{n+1}} + \Omega'_{vf} \tag{13}$$

The superscript * denotes the predicted value; the superscript n and $n + 1$ refers to the variables at the known and unknown time levels; the subscript i and j denote the grid in x- and y-directions; and, Ω'_{hf}, Ω'_{uf} and Ω'_{vf} are the functions of the known value of variables h, u, v at the time level n.

The backward finite-difference is used to calculate the water depth h by the continuity equation (Equation (1)) and the u and v are computed by the momentum equations (Equations (2) and (3)). The corrected value may be written as:

$$h_{i,j}^{**} = h_{i,j}^{n} + \Omega'_{hb} \tag{14}$$

$$u_{i,j}^{**} = u_{i,j}^{n} \frac{h_{i,j}^{n}}{h_{i,j}^{n+1}} + \Omega'_{ub} \tag{15}$$

$$v_{i,j}^{**} = v_{i,j}^{n} \frac{h_{i,j}^{n}}{h_{i,j}^{n+1}} + \Omega'_{vb} \tag{16}$$

The superscript ** denotes the corrected value; Ω'_{hb}, Ω'_{ub}, and Ω'_{vb} are the functions of the known value of variables h, u, v at the time level n.

The value of the variables at the unknown time level could be calculated by the predicted and corrected values that may be written as:

$$h_{i,j}^{n+1} = \frac{1}{2}\left(h_{i,j}^{*} + h_{i,j}^{**}\right) \tag{17}$$

$$u_{i,j}^{n+1} = \frac{1}{2}\left(u_{i,j}^{*} + u_{i,j}^{**}\right) \tag{18}$$

$$v_{i,j}^{n+1} = \frac{1}{2}\left(v_{i,j}^{*} + v_{i,j}^{**}\right) \tag{19}$$

Bed Evolution Model—MacCormack Explicit Finite—Difference Method

The explicit finite-difference method is used to discretize the suspended sediment concentration convection-diffusion equation (Equation (5)) and the continuity equation for bed elevation variations (Equation (10)) to calculate the volumetric concentration of suspended sediments and bed elevation. The volumetric concentration of suspended sediments C is calculated by:

$$C_{i,j}^{n+1} = \frac{C_{i,j}^{n}\, h_{i,j}^{n}}{h_{i,j}^{n+1}} + \Omega'_{c} \tag{20}$$

where Ω'_c is composed of the known value of variables h, u, v, C at the time level n.

The bed elevation may be written as:

$$z_{i,j}^{n+1} = z_{i,j}^{n} + \Omega'_{z} \tag{21}$$

where Ω'_z is composed of the known value of variables h, u, v, C at the time level n.

3. Study Area

A-Gong-Dian Reservoir (Figure 1) is used as an illustrative example in this study. This reservoir, located in Kaohsiung City, (southern Taiwan), collects water from Joushui River and Wanglai River. The total watershed area is 29.58 with 12.81 km^2 (43%) from Joushui River watershed and 16.77 km^2 (57%) from Wanglai River watershed. The length of the dam is 2.38 km, making it the longest dam in Taiwan. Its major purpose is flood control, while other uses, such as irrigation, water supply, and tourism benefit.

The elevation of the dam top, design water level, and maximum water level are 42, 37, and 40 m, respectively. The reservoir was completed in 1953. However, since its completion, large amounst of green-grey clay and yellow silty clay from the upstream watersheds of Joushui and Wanglai rivers have been washed into the reservoir and severe sedimentation has been observed [37]. The effective reservoir capacity was slashed from 20.5 to 5.9 million cubic meters in 1996. In order to revamp the reservoir, the A-Gong-Dian reservoir improvement project was implemented in 1997. Large-scale sediment flushing of the reservoir was executed and 11.6 million cubic meters of sediments were dredged, and the reservoir reached empty storage. The reservoir improvement project involved dam improvement, conduit spillway reconstruction, water intake tower reconstruction, trans-basin waterway, etc. It was finally completed in 2005, and re-opened in June 2006. The shaft spillway pipe (Figure 2) has been operated ever since, for the period 1 June to 10 September annually, which corresponds to the wet season in this region.

Although its design capacity storage is 20.5 million cubic meters, currently, the effective storage capacity is 16.69 million cubic meters, and the total water storage is 45 million cubic meters. The reservoir adopts a shaft spillway pipe having a 2.8 m diameter to reduce the pipe top elevation to 27 m. Based on hydraulic model test, flow discharge of the shaft spillway pipe can be expressed by Equations (22) and (23) [37]:

$$\text{Free overfall } Q_{\text{out}} = 34.12(H_s - 27)^{1.5},\ H_s \leq 28.57 \text{ m} \tag{22}$$

$$\text{Pipe flow } Q_{out} = 17.63(H_s - 14)^{0.5},\ H_s > 28.57 \text{ m} \tag{23}$$

where H_s is water level in the reservoir, Q_{out} is the releasing discharge. The maximum releasing discharge of pipe flow for the shaft spillway pipe is 89.90 m^3/s when the water level reaches the 40-m design maximum flood retention level.

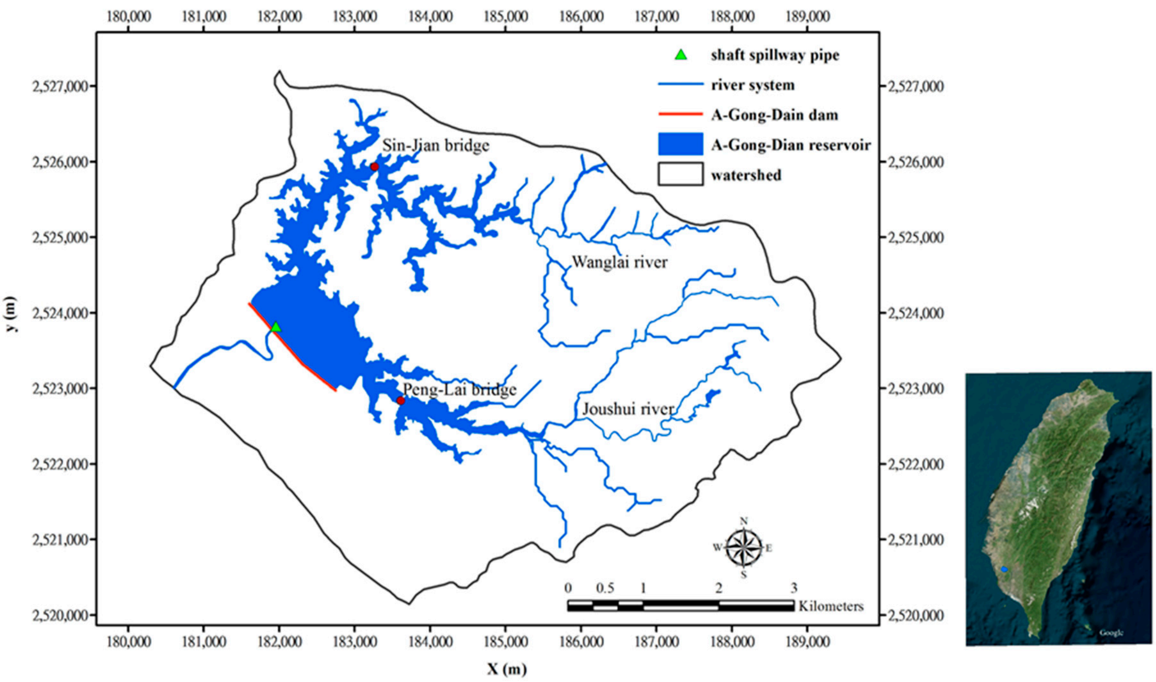

Figure 1. A-Gong-Dian Reservoir watershed and its river system.

Figure 2. Shaft spillway pipe.

4. Methodology

In order to understand the sedimentation pattern, distribution of sediments into the A-Gong-Dian reservoir, bed evolution within the reservoir, and the sediment flushing efficiency of an empty storage operation of the shaft spillway pipe during a flood season, a depth-averaged two-dimensional bed evolution model was developed and applied. The upstream boundary condition hydrographs of inflow discharge and suspended sediment concentration for the two-dimensional bed evolution model were calculated by the PSED model [26,38].

The PSED model can accurately estimate discharge hydrographs, sediment hydrograph, suspended sediment transport rate, and sediment yield from a watershed. In this model, GIS is used to partition the river catchment into computed river cells and land cells, according to the spatial distribution of the physiographical characteristics, such as topography, landform, and vegetation distribution in the watershed. Due to the complex nature of these earth features, a large amount of data is often generated. With the assistance of GIS, the PSED model can handle enormous hydrologic and physiographic datasets, simulating the physical erosion process without the need for simplification.

Computations were done for the storage region between Sin-Jian Bridge of the Wanglai river and the Peng-Lai Bridge of the Joushui river, which is about 5 km long. Cross-sections were measured by the Southern Water Resources Bureau in 2008, and the measured elevations are shown in Figure 3. The study area was discretised into 26,251, squared, $\Delta x = \Delta y = 10$ m, computational cells and the time step was 0.05 s (Δt = 0.05). Conducted field experiments have shown the average sediment particle size to be 0.015 mm, while the Manning's roughness coefficient was 0.028. The initial water depth condition was 0.1 m, while velocity and sediment concentration were 0 for each computed grid.

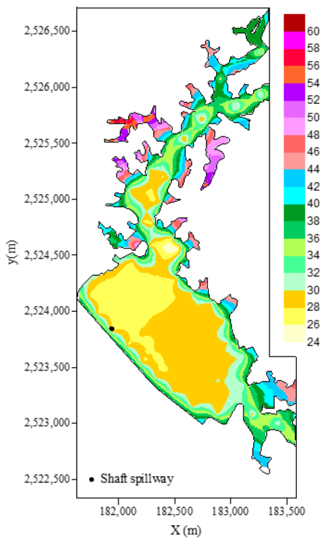

Figure 3. Bed elevation in storage area of A-Gong-Dian reservoir.

The hydrograph boundary conditions of inflow discharge and suspended sediment concentration for the typhoon event and design rainfall of one- and two-day storms under various return periods (2, 5, 10, 25, 50, 100, 200-year) for the depth-averaged two-dimensional bed evolution model were simulated and calculated by the PSED model.

5. Results and Discussions

5.1. Analysis of the Sediment Flushing Efficiency of an Empty Storage

Reducing sediment deposition to increase flood control volume is crucial for Agongdian reservoir. Therefore, sediment flushing of empty storage by a shaft spillway pipe is operated during the wet period to decrease the sediment deposition within the reservoir bed. To understand the sediment flushing efficiency of empty storage by a shaft spillway pipe under one-day and two-day storms of various return periods, the operations for sediment flushing of the empty storage were simulated using the depth-averaged two-dimensional bed evolution model, and the results are shown in Tables 1 and 2.

The results indicate that the average sediment flushing efficiency for one-day and two-day storms are close, 58.50% and 59.39%, respectively. For the simulated storms, the lowest efficiencies are 58.16%, 58.62% (200-year return period), and the highest efficiencies are 58.98%, 60.19% (10-year, 2-year return period). The simulation results are close to 65.34% [39], which agree well with the efficiency obtained from the hydraulic model test in the laboratory. The results show that the two-dimensional bed evolution model can reasonably simulate sediment flushing of empty storage by a shaft spillway pipe, as sediment flushing efficiency reached up to 60%.

Table 1. Empty flushing efficiency in one-day storms under different return periods.

Return Period (Year)	Sediment Yield of the Watershed (m^3)	Sediment Deposited in the Reservoir (m^3)	Sediment Flushing by Shaft Spillway (m^3)	Sediment Flushing Efficiency (%)
2	201,341	83,154	118,187	58.70
5	280,522	116,875	163,647	58.34
10	331,857	136,121	195,736	58.98
25	375,159	156,963	218,196	58.16
50	427,718	176,549	251,169	58.72
100	464,325	193,141	271,184	58.40
200	498,867	208,575	290,292	58.16

Table 2. Empty flushing efficiency in two-day storms under different return periods.

Return Period (Year)	Sediment Yield of the Watershed (m^3)	Sediment Deposited in the Reservoir (m^3)	Sediment Flushing by Shaft Spillway (m^3)	Sediment Flushing Efficiency (%)
2	284,238	113,155	171,083	60.19
5	397,096	159,791	237,305	59.76
10	471,082	189,846	281,236	59.70
25	541,196	220,050	321,146	59.34
50	625,933	255,506	370,427	59.18
100	701,485	287,889	413,596	58.96
200	775,718	320,992	454,726	58.62

5.2. Analysis of Sediment Delivery Behaviour in Reservoirs

Sediment flushing efficiency is related to the life and function of the reservoir. Therefore, this topic of great importance for reservoir management. In addition, it is necessary to carry out the analysis from sediment transport into the reservoir to bed evolution during the process of flooding and sediment flushing. Management of reservoirs does not only entail improving the flushing efficiencies, but in depth investigations are needed to understand the whole process from catchment erosion, to sediment transport and bed evolution, and finally to the removal of the sediments. To understand the whole complex process of sediments transport during heavy storms or floods in a reservoir, the severe storm event typhoon Morakot, which hit Taiwan in 6 to 10 August 2009, was numerically simulated to estimate the variations of water depth, suspended sediment concentration, sediment delivery, and bed evolution. Results are shown in Figures 4–6. Figure 4 show water depth variation in the reservoir at 36, 60, 72, 84, 96, and 120-h, while Figure 5 show distribution of suspended sediment concentration, and Figure 6, bed evolution.

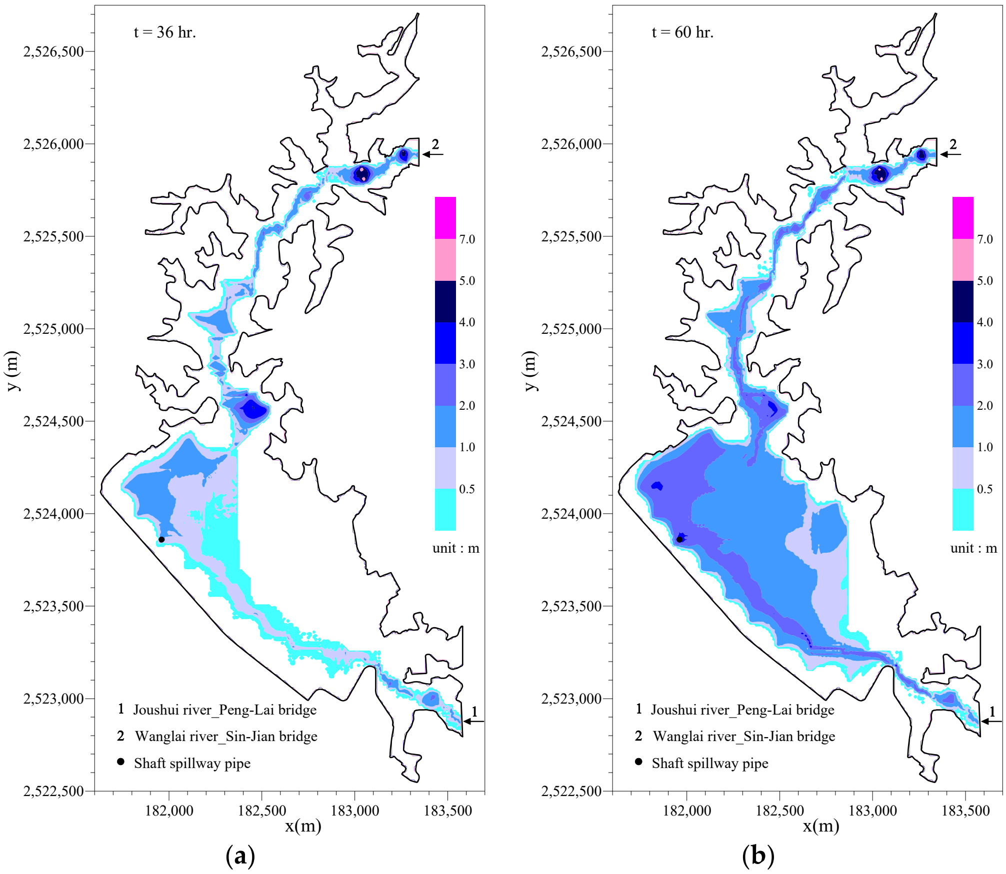

Figure 4. *Cont.*

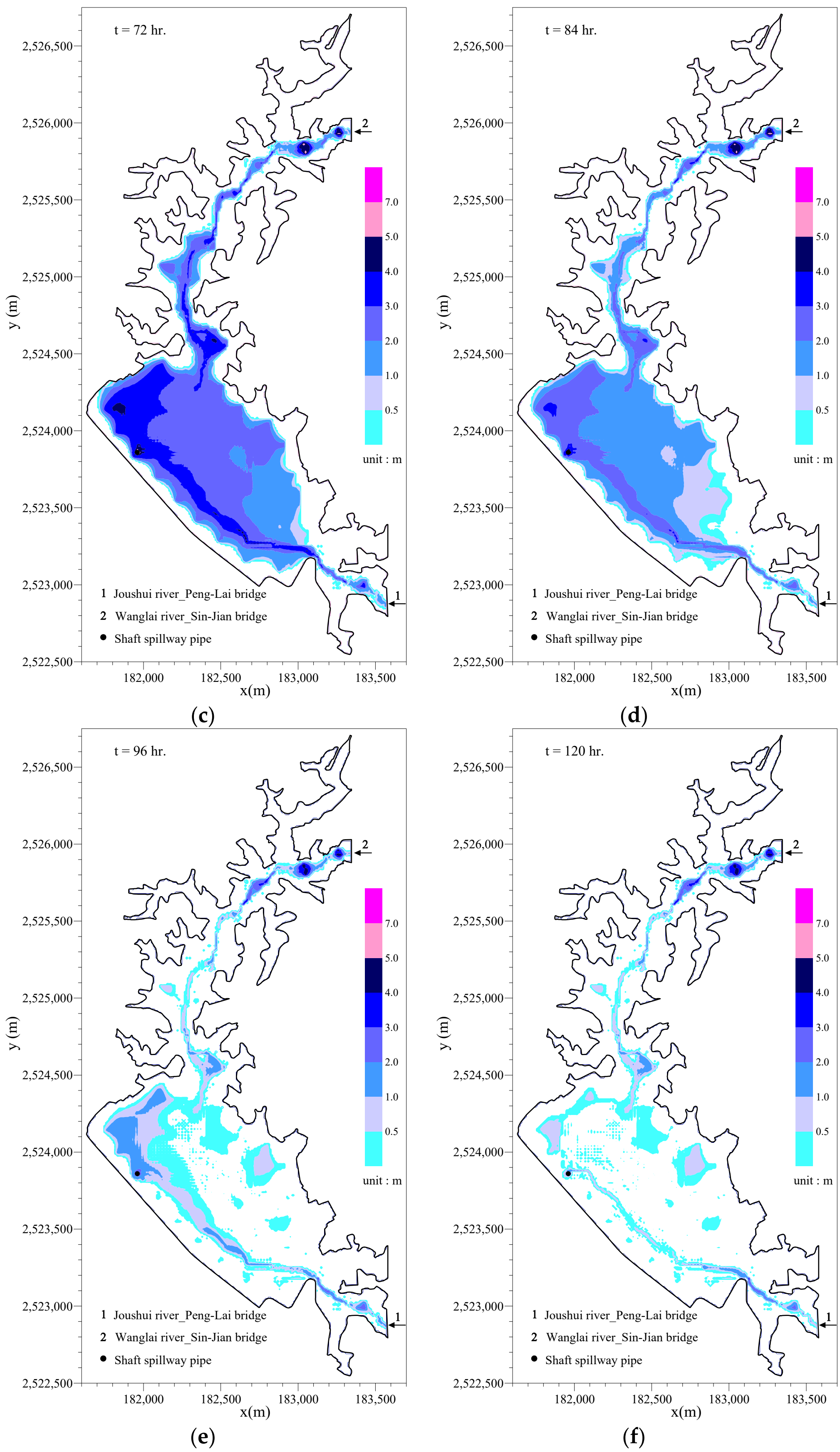

Figure 4. (**a**) Water depth in the reservoir at t = 36 h; (**b**) Water depth in the reservoir at t = 60 h; (**c**) Water depth in the reservoir at t = 72 h; (**d**) Water depth in the reservoir at t = 84 h; (**e**) Water depth in the reservoir at t = 96 h; and, (**f**) Water depth in the reservoir at t = 120 h.

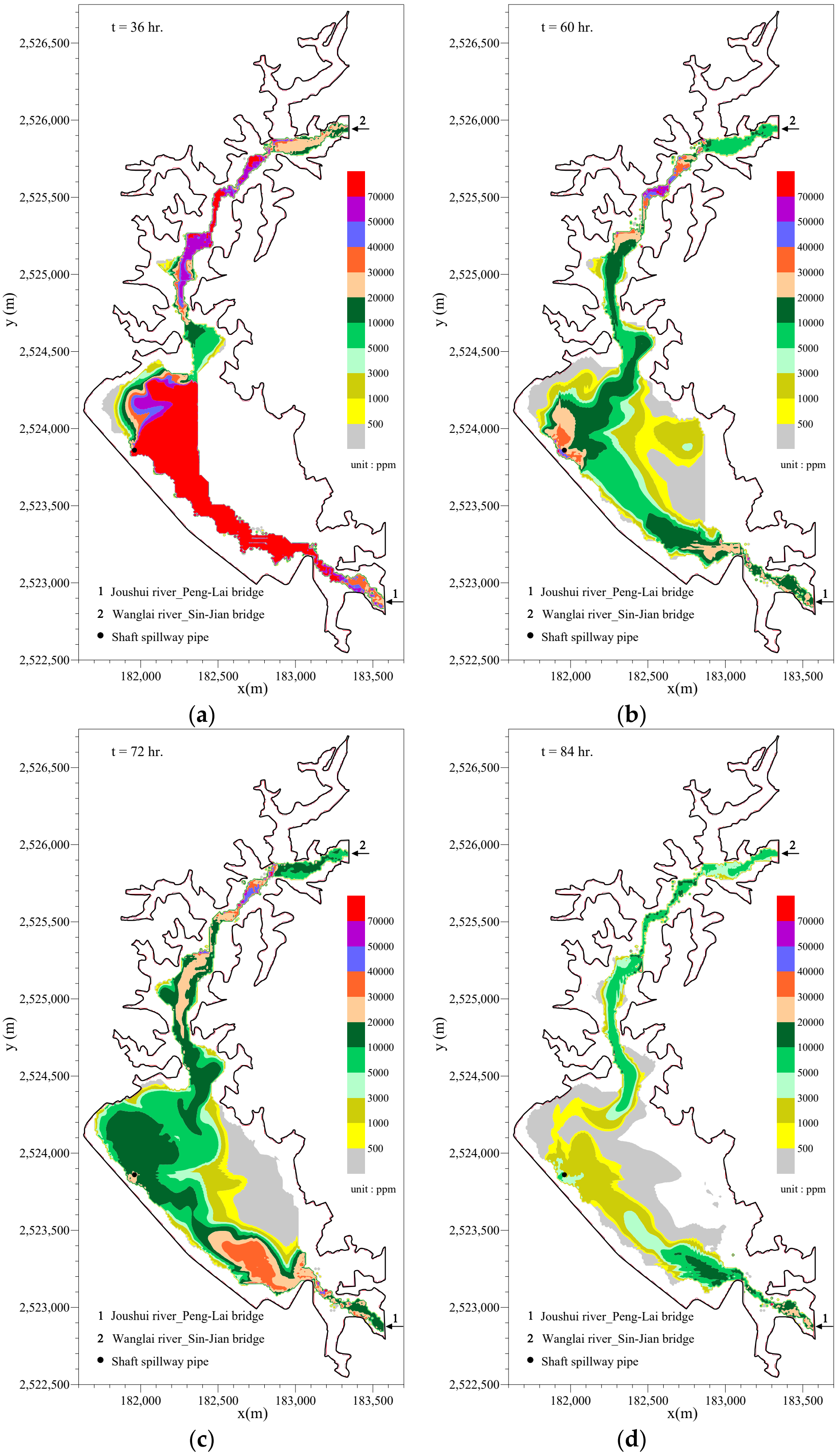

Figure 5. *Cont.*

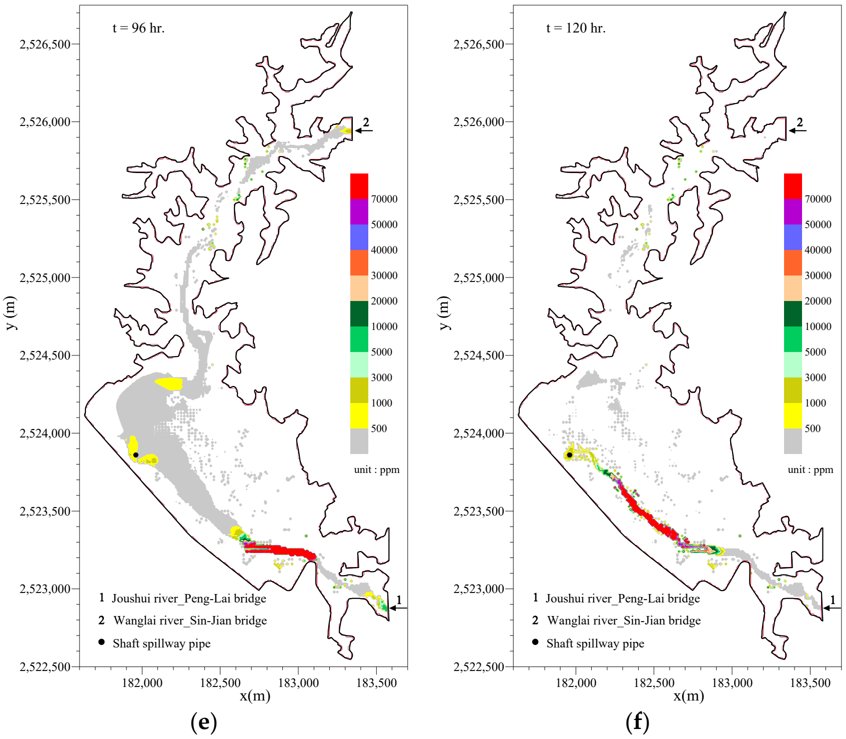

Figure 5. (**a**) Distribution of suspended sediment concentration at t = 36 h; (**b**) Distribution of suspended sediment concentration at t = 60 h; (**c**) Distribution of suspended sediment concentration at t = 72 h; (**d**) Distribution of suspended sediment concentration at t = 84 h; (**e**) Distribution of suspended sediment concentration at t = 96 h; and, (**f**) Distribution of suspended sediment concentration at t = 120 h.

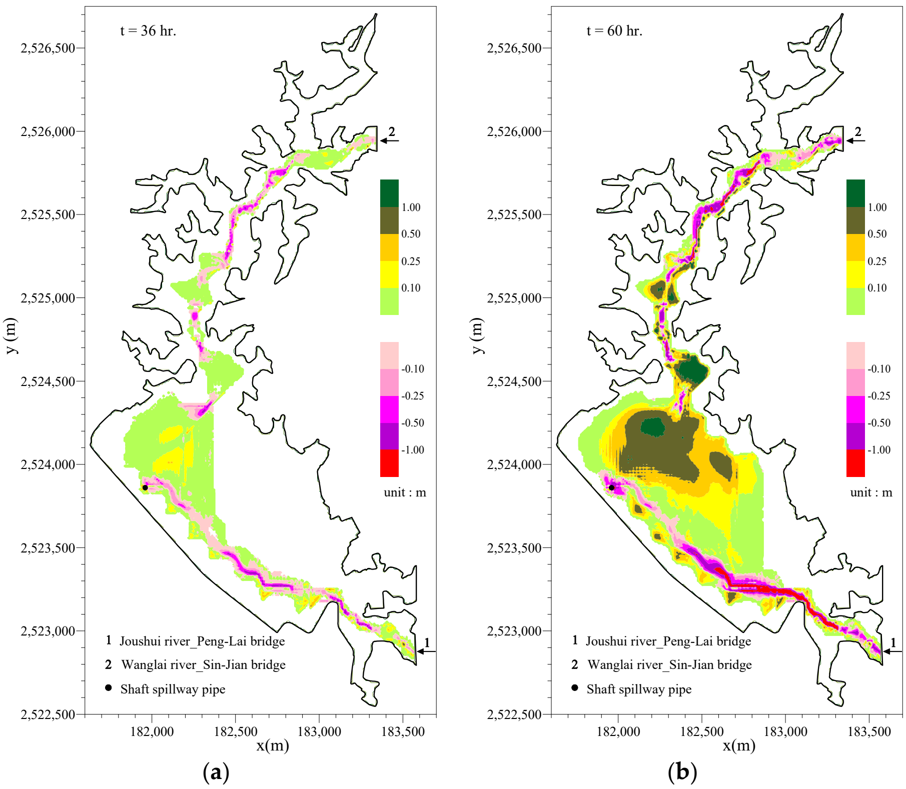

Figure 6. *Cont.*

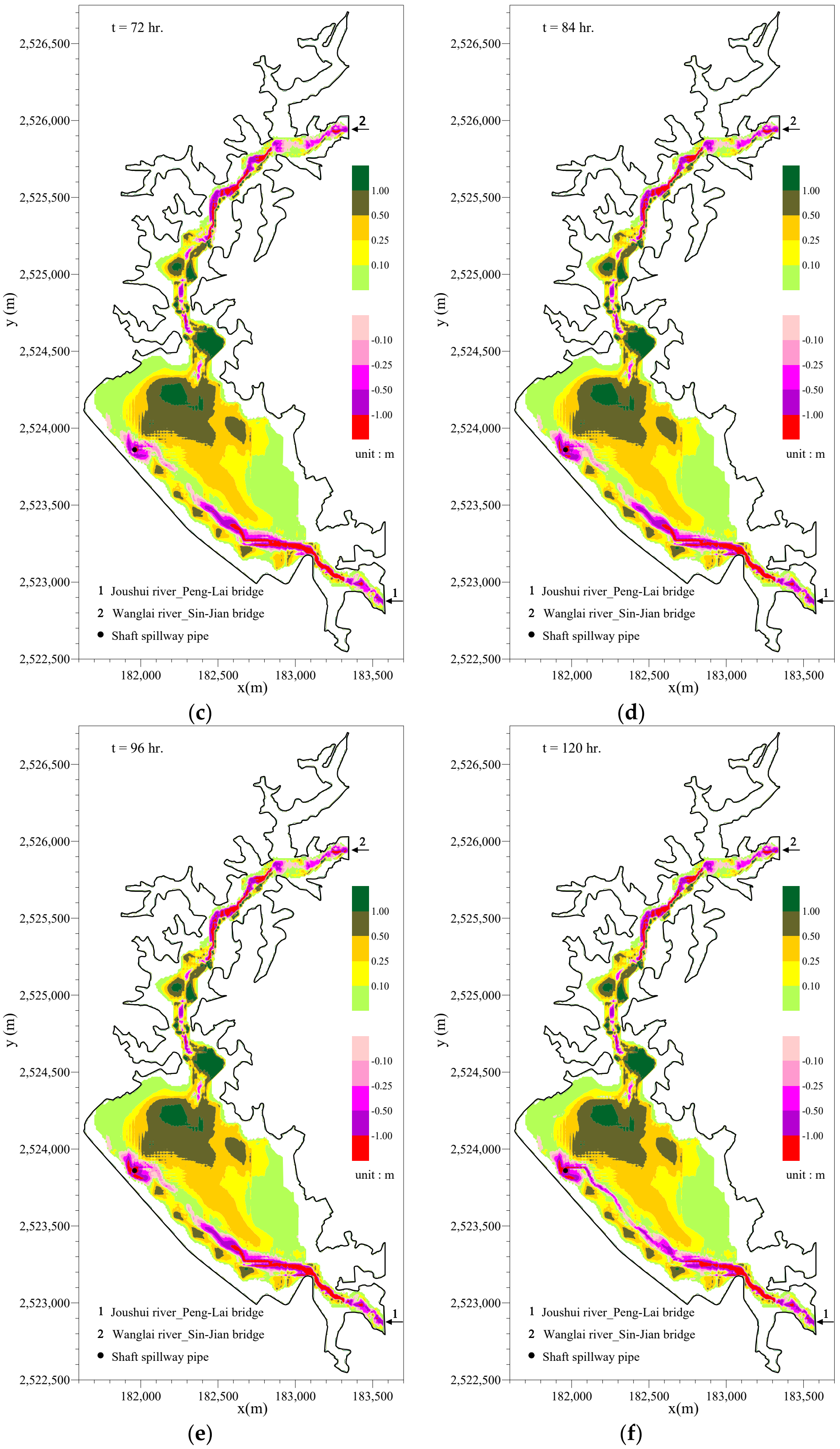

Figure 6. (**a**) Bed evolution in the reservoir at t = 36 h; (**b**) Bed evolution in the reservoir at t = 60 h; (**c**) Bed evolution in the reservoir at t = 72 h; (**d**) Bed evolution in the reservoir at t = 84 h; (**e**) Bed evolution in the reservoir at t = 96 h; and, (**f**) Bed evolution in the reservoir at t = 120 h.

Water depth is shown to initially increase in Figure 4 while flow entered the reservoir, and after t = 72-h it began to gradually decrease as the inflow discharge became less than the releasing discharge of the shaft spillway. Figure 5 shows the distribution of suspended sediment concentration. The results show muddy water into the reservoir and convection-diffusion of sediment in the reservoir. In addition, the high bed shear stress that was caused by the increased velocity entrained more sediments into the flow, thus the high turbid flow in the reservoir. Sediment concentration reached more than 70,000 ppm and the high turbid flow was released by the shaft spillway pipe, and the siltation in the reservoir was due to the unreleased turbid flow.

Figure 6 shows both the erosion and the deposition depth during typhoon Morakot. Erosion is seen to be more dominant at the thalweg (>0.5 m), and is more apparent at the erosion ditch that is generated between Joushui river and the shaft spillway. This could be attributed to the high flow velocity, resulting from the shaft spillway pipe, and the steep slopes around this area. Moreover, a not significant erosion ditch is seen between the Wanglai river and the shaft spillway pipe. Deposition is prevalent from the 60th hour, especially downstream of the Wanglai river, greater than 0.5 m, and is not severe from the Joushui side as it hardly reaches 0.25 m. It is worth mentioning that the downstream of Wanglai river where it joins the reservoir is wider (Figure 2) when compared to the Joushui river, hence the flow velocity is greatly reduced and it increases the rate of sediment deposition. Part of the sediments deposited in the reservoir could not be flushed out by the shaft spillway pipe, resulting in erosion-deposition interplay.

Final bed evolution under the different return periods of one and two-day storms, with a total simulation time of 120 h is shown in Figures 7–13. Similar patterns of erosion and deposition are seen with the different return periods; moreover, these intensify with increasing the return period. There is a significant erosion ditch (>1 m) from the Joushui river down to all around the shaft spillway pipe. The maximum deposition area in the north-eastern of the shaft spillway pipe is mainly due to the non-significant erosion ditch that is seen between the Wanglai river and the shaft spillway pipe. Hence, if the shaft spillway pipe were shifted to the applicable distance in the north-eastern direction, it will improve the probability of forming an erosion ditch between Wanglai river and the shaft spillway. There would be two significant erosion ditches formed to enhance flushing.

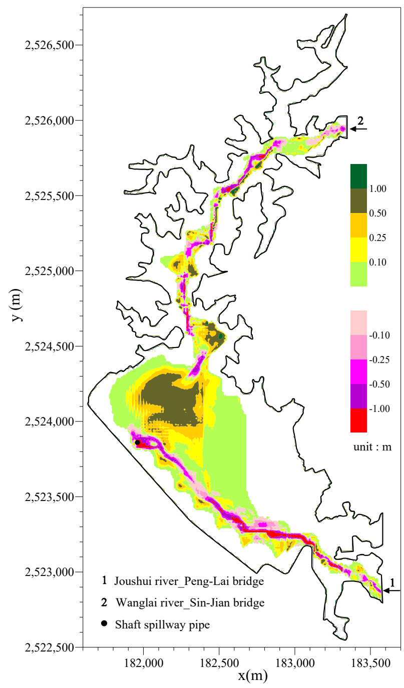

Figure 7. Bed evolution in the reservoir during a two-year return period, t = 120 h.

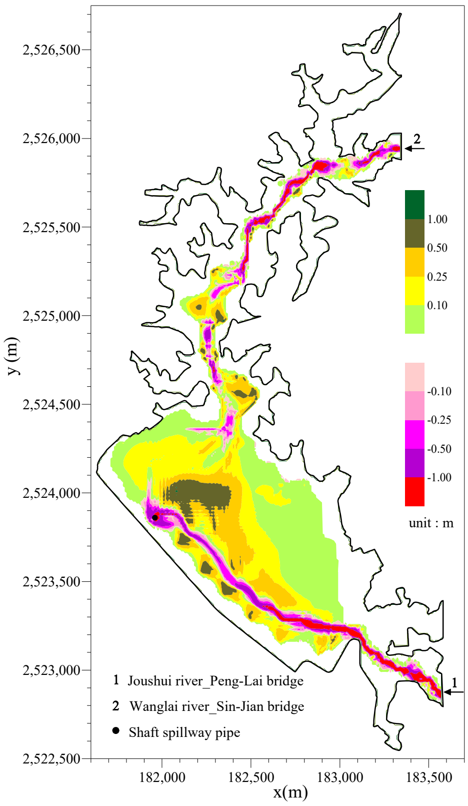

Figure 8. Bed evolution in the reservoir during a five-year return period, t = 120 h.

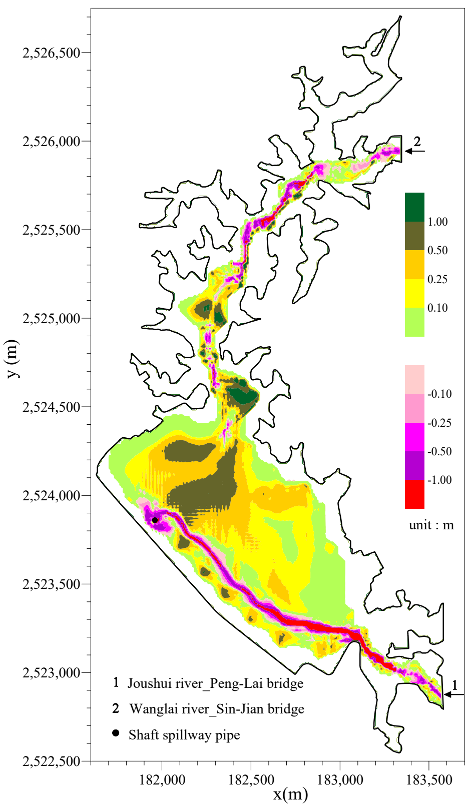

Figure 9. Bed evolution in the reservoir during a 10-year return period, t = 120 h.

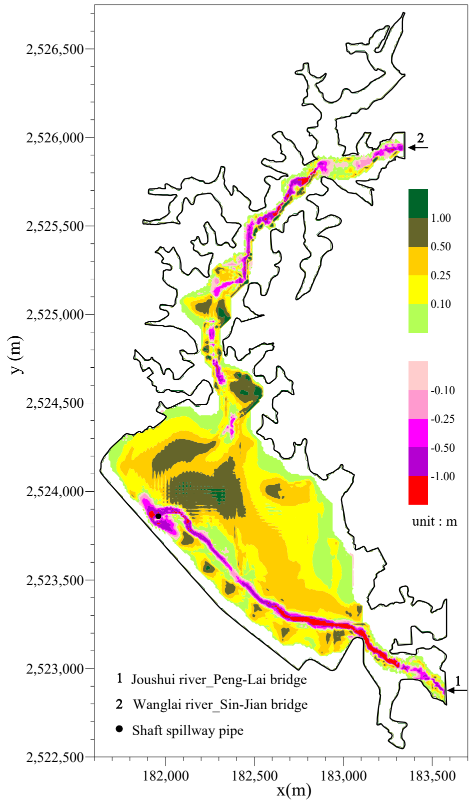

Figure 10. Bed evolution in the reservoir during a 25-year return period, t = 120 h.

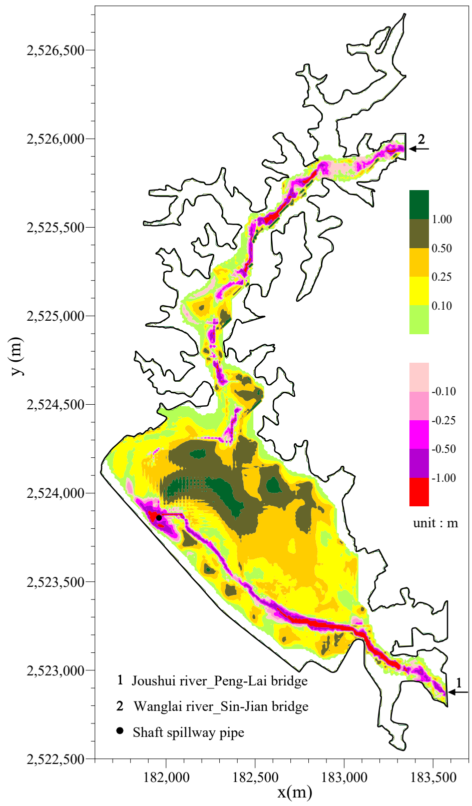

Figure 11. Bed evolution in the reservoir during a 50-year return period, t = 120 h.

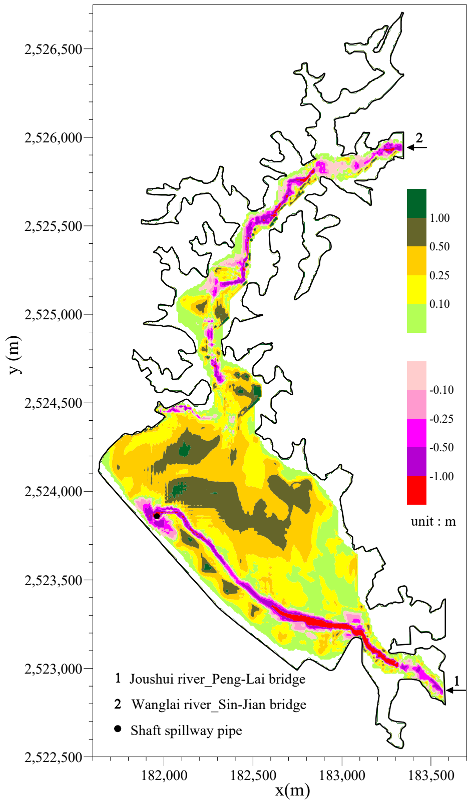

Figure 12. Bed evolution in the reservoir during a 100-year return period, t = 120 h.

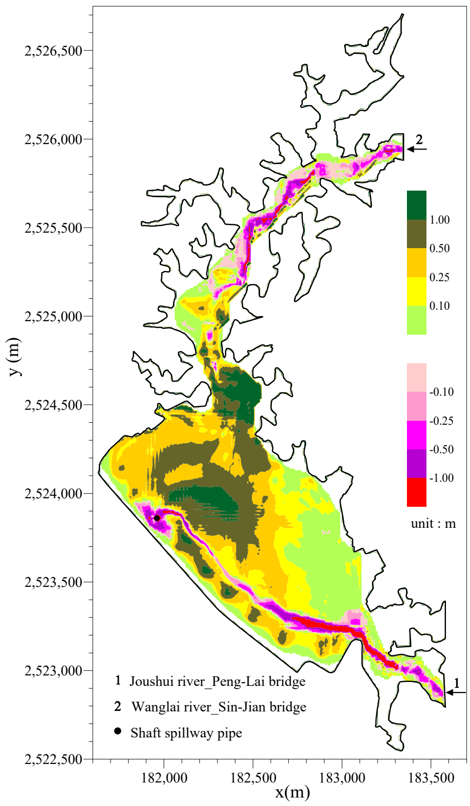

Figure 13. Bed evolution in the reservoir during a 200-year return period, t = 120 h.

6. Conclusions

A model is developed and applied to the simulation of sediment erosion/deposition and sediment distribution within a reservoir, and to simulate the flushing efficiency of a shaft spillway pipe. Hydrograph boundary conditions of inflow and suspended sediment concentration of one-day and two-day storms of different return periods, (2, 5, 10, 25, 50, 100, 200-year), were computed by the 1D, PSED model. Based on the results, the following conclusions may be drawn.

The average efficiency of the empty flushing by a shaft spillway pipe under one- and two-day storms of various return periods were almost similar, 58.49% and 59.39%, respectively. These results were found to be adequate as the efficiency was almost 60%. The overall simulation results are close to 65.34%, which is the efficiency that is obtained from a hydraulic model test in a laboratory.

Bed evolution in the reservoir was significantly driven by flow velocity under empty flushing by the shaft spillway pipe after the rainfall had stopped. A significant erosion ditch was generated after 96 h of simulation time between Joushui river and the shaft spillway pipe. At the end of the simulation time, no erosion ditch was developed from the Wanglai river due to the relatively wider cross section and low flow velocity. The shaft spillway could not completely flush out the sediments that were deposited; as a result, bed evolution was a mixture of erosion and deposition. Similar patterns of erosion and deposition were observed for the selected storm, typhoon Morakot, and the design rainfall events under different return periods.

A common observation was the significant erosion ditch that formed between the Wanglai river and the shaft spillway pipe that enhanced flushing. From our findings, we propose a relocation of the shaft spillway pipe towards the north-eastern direction. Shifting the pipe to this direction could improve the probability of forming the erosion ditch between Wanglai river and the shaft spillway. Two significant erosion ditches would improve the empty flushing efficiency even further.

Acknowledgments: Observed and hydraulic model test data for this study was provided by A-Gong-Dian Reservoir Management Centre, Southern Region Water Resources office, Water Resources Agency, Ministry of Economic Affairs. The authors gratefully acknowledge their support.

Author Contributions: Ching-Nuo Chen conceived and designed the study and further wrote the manuscript while Chih-Heng Tsai contributed significantly with data analysis.

Conflicts of Interest: The authors declare no conflict of interest.

References

1. Wang, Z.-Y.; Hu, C. Strategies for Managing Reservoir Sedimentation. *Int. J. Sediment Res.* **2009**, *24*, 369–384. [CrossRef]
2. Schleiss, A.J.; Boes, R.M. *Dams and Reservoirs under Changing Challenges*; CRC Press: Boca Raton, FL, USA, 2011.
3. Kondolf, G.M.; Gao, Y.; Annandale, G.W.; Morris, G.L.; Jiang, E.; Zhang, J.; Cao, Y.; Carling, P.; Fu, K.; Guo, Q. Sustainable Sediment Management in Reservoirs and Regulated Rivers: Experiences from Five Continents. *Earth Future* **2014**, *2*, 256–280. [CrossRef]
4. Chang, F.-J.; Lai, J.-S.; Kao, L.-S. Optimization of Operation Rule Curves and Flushing Schedule in a Reservoir. *Hydrol. Process.* **2003**, *17*, 1623–1640. [CrossRef]
5. Emamgholizadeh, S.; Samadi, H. Desilting of Deposited Sediment at the Upstream of the Dez Reservoir in Iran. *J. Appl. Sci. Environ. Sanit.* **2008**, *3*, 25–35.
6. Chaudhry, M.A.; Habib-ur-Rehman, M.; Akhtar, M.N.; Hashmi, H.N. Modeling Sediment Deposition and Sediment Flushing through Reservoirs Using 1-D Numerical Model. *Arab. J. Sci. Eng.* **2014**, *39*, 647–658. [CrossRef]
7. Castillo, L.G.; Carrillo, J.M.; Álvarez, M.A. Complementary Methods for Determining the Sedimentation and Flushing in a Reservoir. *J. Hydraul. Eng.* **2015**, *141*, 05015004. [CrossRef]
8. Basson, G.R.; Rooseboom, A. Sediment Pass-through Operations in Reservoirs. In Proceedings of the International Conference on Reservoir Sedimentation, Fort Collins, CL, USA, 9–13 September 1996; pp. 1107–1130.

9. Madadi, M.R.; Rahimpour, M.; Qaderi, K. Improving the Pressurized Flushing Efficiency in Reservoirs: An Experimental Study. *Water Resour. Manag.* **2017**, *31*, 4633–4647. [CrossRef]
10. Morris, G.L.; Fan, J. *Reservoir Sedimentation Handbook: Design and Management of Dams, Reservoirs, and Watersheds for Sustainable Use*; McGraw-Hill: New York, NY, USA, 1998.
11. United States Society on Dams. *Modeling Sediment Movement in Reservoirs*; United States Society on Dams: Denver, CO, USA, 2015.
12. Basson, G.R.; Rooseboom, A. *Dealing with Reservoir Sedimentation: Guidelines and Case Studies*; International Commission on Large Dams: Paris, France, 1996.
13. Pagliari, D.; Rossi, L.; Passoni, D.; Pinto, L.; De Michele, C.; Avanzi, F. Measuring the Volume of Flushed Sediments in a Reservoir Using Multi-Temporal Images Acquired with Uas. *Geomat. Nat. Hazards Risk* **2017**, *8*, 150–166. [CrossRef]
14. Su, T.-C.; Chou, H.-T. Application of Multispectral Sensors Carried on Unmanned Aerial Vehicle (Uav) to Trophic State Mapping of Small Reservoirs: A Case Study of Tain-Pu Reservoir in Kinmen, Taiwan. *Remote Sens.* **2015**, *7*, 10078–10097. [CrossRef]
15. Guertault, L.; Camenen, B.; Peteuil, C.; Paquier, A. Long Term Evolution of a Dam Reservoir Subjected to Regular Flushing Events. *Adv. Geosci.* **2014**, *39*, 89–94. [CrossRef]
16. Chou, F.N.F.; Wu, C.W. Assessment of Optimal Empty Flushing Strategies in a Multi-Reservoir System. *Hydrol. Earth Syst. Sci. Discuss* **2016**, *2016*, 1–49. [CrossRef]
17. U.S. Army Corps of Engineers. *Hec-6 Scour and Deposition in Rivers and Reservoir, User's Manual*; Hydrologic Engineering Centre: Davis, CA, USA, 1991.
18. U.S. Army Corps of Engineers. *Hec-Ras (Hydrologic Engineering Center River Analysis System) Manual*; Hydrologic Engineering Centre: Davis, CA, USA, 2005.
19. Chang, H.H. *Fluvial Processes in River Engineering*; Wiley: Hoboken, NJ, USA, 1988.
20. Chang, H.H.; Harrison, L.L.; Lee, W.; Tu, S. Numerical Modeling for Sediment-Pass-through Reservoirs. *J. Hydraul. Eng.* **1996**, *122*, 381–388. [CrossRef]
21. Olsen, N.R.B. Two-Dimensional Numerical Modelling of Flushing Processes in Water Reservoirs. *J. Hydraul. Res.* **1999**, *37*, 3–16. [CrossRef]
22. Olsen, N.R.B.; Skoglund, M. Three-Dimensional Numerical Modeling of Water and Sediment Flow in a Sand Trap. *J. Hydraul. Res.* **1994**, *32*, 833–844. [CrossRef]
23. Fang, H.-W.; Rodi, W. Three-Dimensional Calculations of Flow and Suspended Sediment Transport in the Neighborhood of the Dam for the Three Gorges Project (Tgp) Reservoir in the Yangtze River. *J. Hydraul. Res.* **2003**, *41*, 379–394. [CrossRef]
24. Khosronejad, A.; Rennie, C.D.; Neyshabouri, A.A.S.; Gholami, I. Three-Dimensional Numerical Modeling of Reservoir Sediment Release. *J. Hydraul. Res.* **2008**, *46*, 209–223. [CrossRef]
25. Wang, Y.M.; Tfwala, S.S.; Chan, H.C.; Lin, Y.C. The Effects of Sporadic Torrential Rainfall Events on Suspended Sediments. *Arch. Sci. J.* **2013**, *66*, 211–224.
26. Chen, C.-N.; Tsai, C.-H.; Tsai, C.-T. Simulation of Sediment Yield from Watershed by Physiographic Soil Erosion–Deposition Model. *J. Hydrol.* **2006**, *327*, 293–303. [CrossRef]
27. Tsai, C.H.; Tsai, C.T. Simulation of Two-Dimensional Gradually-Varied Unsteady Flow in Curved Channels. *J. Chin. Inst. Civ. Hydraul. Eng.* **1995**, *7*, 461–473.
28. Tsai, C.H. Numerical Simulation of Flow and Bed Evolution in Alluvial River with Levees. Ph.D. Thesis, National Cheng-Kung University, Tainan, Taiwan, 2000.
29. Itakura, T.; Kishi, T. Open Channel Flow with Suspended Sediments. *J. Hydraul. Div.* **1980**, *106*, 1325–1343.
30. Shimizu, Y.; Yamaguchi, H.; Itakura, T. Three-Dimensional Computation of Flow and Bed Deformation. *J. Hydraul. Eng.* **1990**, *116*, 1090–1108. [CrossRef]
31. Meyer-Peter, P.E.; Muller, R. Formulas for Bedload Transport. In Proceedings of the 2nd International Association for Hydraulic Research, Stockholm, Sweden, 7–9 June 1948; pp. 39–64.
32. Wong, M.; Parker, G. Reanalysis and Correction of Bed-Load Relation of Meyer-Peter and Müller Using Their Own Database. *J. Hydraul. Eng.* **2006**, *132*, 1159–1168. [CrossRef]
33. Paola, C.; Voller, V.R. A Generalized Exner Equation for Sediment Mass Balance. *J. Geophys. Res. Earth Surf.* **2005**, *110*, 2156–2202. [CrossRef]
34. Parker, G.; Paola, C.; Leclair, S. Probabilistic Exner Sediment Continuity Equation for Mixtures with No Active Layer. *J. Hydraul. Eng.* **2000**, *126*, 818–826. [CrossRef]

35. Komura, S.; Simons, D.B. River-Bed Degradation Below Dams. *J. Hydraul. Div.* **1967**, *93*, 1–14.
36. Bhallamudi, M.S.; Chaudhry, H.M. Computation of Flows in Open-Channel Transitions. *J. Hydraul. Res.* **1992**, *30*, 77–93. [CrossRef]
37. Southern Water Resources Bureau. *Effect Assessment of Empty Storage Operation for Sediment Prevention Observation Program of Agongdian Reservoir*; Water Resources Agency, MOEA: Taichung, Taiwan, 2010.
38. Chen, C.-N.; Tsai, C.-H. The Impact of Climate Change on Inundation Potential. *Int. J. Environ. Sci. Dev.* **2013**, *4*, 496–500. [CrossRef]
39. Water Resources Planning Institute. *Hydraulic Model Studies on the Functions and Operations of Silting Prevention in a-Kung-Tien Reservior*; Water Resources Agency, Ministry of Economic Affairs: Taichung, Taiwan, 2003.